

A SECOND GENERATION LIGHT SOURCE AIMING AT HIGH POWER ON THE GIANT DIPOLE RESONANCE

X. Buffat*, L.L. Cuanillion and E. Kneubuehler, CERN, Geneva, Switzerland

Abstract

We propose an alternative to nuclear waste transmutation and energy amplification using a second generation light source rather than a high power proton beam. The main parameters of the ring and insertion devices are estimated, targeting a photon beam power of 1 GW with a spectrum that maximizes the potential for nuclear reactions via the Giant Dipole Resonance. The synergies with technologies developed for high energy physics, in particular within the Future Circular Collider study (FCC), are highlighted.

INTRODUCTION

The usage of high power proton beams for the transmutation of nuclear waste from conventional reactors as well as for waste-less nuclear energy production is an active field of research since its initial proposal [1, 2]. Here we study an alternative approach based on a conventional light source of the second generation, with an insertion consisting of a high field superconducting dipole magnet. Nuclear fission and neutron emission are induced via the Giant Dipole Resonance (GDR) [3]. In the next section, we will determine the beam energy and insertion magnet properties that maximises the radiated power on the GDR. We then describe the design of a synchrotron that operates on this optimum. To conclude, the construction cost and the technologies that could lower it are discussed.

RADIATION SPECTRUM

Let us consider a beam of electrons with a current I_e and an energy E_e . We place a short dipole magnet with field B_i and magnetic length L_i on the beam trajectory. The photon beam power emitted is given by [4]:

$$P_i = I_e L_i \frac{e}{6\pi\epsilon_0} \frac{\beta_r^4 \gamma_r^4}{\rho_i^2}, \quad (1)$$

with e the elementary charge, ϵ_0 the vacuum permittivity and β_r, γ_r the electrons's relativistic factors. The bending radius in the insertion magnet is given by:

$$\rho_i = \frac{m_e \gamma_r \beta_r c}{B_i e}, \quad (2)$$

with m_e the electron mass and c the speed of light. Defining the critical energy as:

$$E_c = \frac{3\hbar c}{2} \frac{\gamma_r^3}{\rho_i} \quad (3)$$

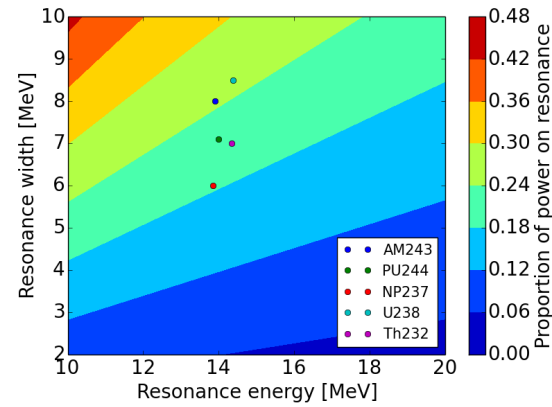
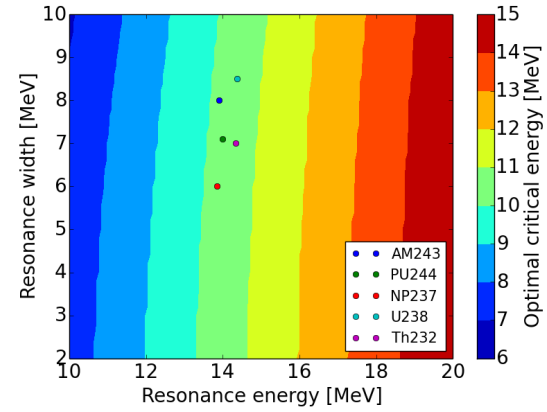


Figure 1: Optimal critical energy (top) and the corresponding proportion of the photon spectrum on the GDR (bottom) as a function of the resonance properties. The values corresponding to the main GDR of a few actinides are shown for reference.

with Planck's constant \hbar , we can write the power spectral density:

$$\frac{dP_i}{d\theta} = \frac{9\sqrt{3}}{8\pi} P_\gamma \theta \int_0^\infty K_{5/3}(x) dx. \quad (4)$$

$K_{5/3}$ is a modified Bessel function and the scaled photon energy is defined by $\theta \equiv E_\gamma/E_c$. This spectrum is rather wide, we are interested in maximising the fraction of the power on the GDR which is roughly given by:

$$\eta_r = \frac{1}{P_i} \int_{\theta_r - \frac{\Delta\theta_r}{2}}^{\theta_r + \frac{\Delta\theta_r}{2}} \frac{dP_i}{d\theta} d\theta, \quad (5)$$

with θ_r the resonance energy and $\Delta\theta_r$ its width scaled by the critical energy. Figure 1 shows the optimal critical energy and the corresponding fraction on the GDR for various

* xavier.buffat@cern.ch

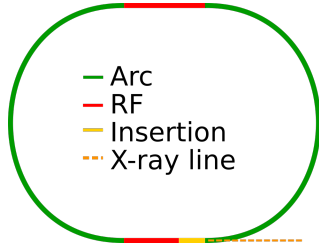


Figure 2: Accelerator layout.

resonance energies and widths. Focusing on the dominant resonance for the photofission of the actinides, a critical energy of 10.5 MeV seems most appropriate yielding a proportion of $\eta_r \approx 20\%$ of the power emitted in the insertion magnet on the GDR. To remain efficient, such an accelerator needs to be coupled with a nuclear reactor. We consider a rough estimate of the rate of photo-nuclear reactions as the rate of photons within the energy range defined in Eq. (5) scaled by the ratio of the GDR cross section σ_{GDR} to the total cross section σ_{tot} :

$$r_r = \frac{P_i \eta_r \sigma_{GDR}}{E_{GDR} \sigma_{tot}} \quad (6)$$

The output power of the coupled accelerator and nuclear reactor is given by:

$$P_{out} = \eta_c \left(P_i + r_r \Delta E + \frac{r_r \eta_n \Delta E}{1-k} \right) - \frac{P_i + P_a}{\eta_{RF}}. \quad (7)$$

The parenthesis contains the energy deposited by the photon beam in the target, the direct production of photo-nuclear reaction with an average release of ΔE as well as the energy amplification by a reactor with criticality k . The neutron yield of the photo-nuclear reactions is η_n . The Carnot efficiency of the thermal power plant is η_c . The power necessary to operate the accelerator is subtracted, taking into account the efficiency of the powering of the cavities η_{RF} . We target a photon power P_i of 1 GW and we assume that the power dissipated in the arcs P_a is 10 times lower, as will be shown in the next section. With a target constituted of natural uranium (i.e. dominated by U238), we have $\sigma_{GDR}/\sigma_{tot} \approx 6\%$, the energy released by photofission is about 200 MeV and the neutron yield is about 2.5 [3]. Coupled to a sub-critical reactor featuring $k = 0.95$, we obtain an output power of 2 GW. While rough, these considerations on the potential of such a setup support further investigations into the design of the required accelerator.

DESIGN

The machine and beam parameters aiming at delivering a photo beam power of 1 GW with a critical energy of 10.5 MeV are listed in Table 1. In the following we describe the rationale for this design.

In order to obtain the optimal critical energy, the beam energy and the insertion magnet field are linked by the fol-

Table 1: Main and Beam Parameters

Beam energy [GeV]	33.0
Total intensity [10^{15}]	1.7
Total current [A]	3.0
Bunch spacing [ns]	2.5
Bunch population [10^{10}]	4.7
Insertion magnet field [T]	14.6
Insertion magnet length [m]	1.1
Photon beam power [GW]	1.0
Total length [km]	26.9
Revolution frequency [kHz]	11.1
Horizontal emittance [nm]	0.6
Emittance Ratio [%]	5
Bunch length [ps]	16
Energy spread [10^{-4}]	6.1
RF phase [$^\circ$]	30
Synchrotron tune	0.21
Dipole filling factor	0.8
Single arc length [km]	12.5
Arc cell length [m]	79.8
Arc cell type	FODO
Phase advance per cell [$^\circ$]	90
Arc SR power density [kW/m]	4.0
Total RF power [GW]	1.1
RF frequency [MHz]	400
Number of cavities	1144
RF filling factor	0.8
RF power per cavity [kW]	962
RF voltage per cavity [kV]	635
RF sections length [km]	1.8
Insertion and spare straights [m]	200.0
Touschek Lifetime [h]	200

lowing relation:

$$E_e = \sqrt{\frac{2\beta_r m_e^3 c^4 E_c}{3\hbar e} \frac{E_c}{B_i}}. \quad (8)$$

Implicitly we have assumed that the beam energy remains constant in the insertion magnet. To meet this hypothesis, we limit the relative energy lost per passage in the insertion magnet to 1%:

$$\frac{eP_i}{I_e} < 0.01E_e. \quad (9)$$

We find that a shorter version (1.1 m) of the prototype high-field dipole magnet that reached 14.6 T with a magnetic length of 1.6 m [5] together with an electron beam of 33 GeV would make a suitable combination. Neglecting the beam size compared to the orbit excursion in the magnet, we find that the diameter of the physical aperture required for the high-field dipole follows

$$d \approx \rho_i - \sqrt{\rho_i^2 - L_i}, \quad (10)$$

which is approximately 8 cm in our design. This is again compatible with the 10 cm of the prototype in [5].

Considering the layout shown in Fig. 2, we seek to determine the dimensions of the different systems. The arc length is mainly constrained by the synchrotron power density in the arcs $\lambda_a = P_a/L_a$, with L_a the total length of the arcs. Considering a dipole filling factor of η_d , the total power emitted in the arcs is given by [4]:

$$P_a = I_e L_a \eta_d \frac{e}{6\pi\epsilon_0} \frac{\beta_r^4 \gamma_r^4}{\rho_a^2}. \quad (11)$$

The beam current is defined by the photon beam power through Eq. (1). Neglecting the impact of the insertion magnet on the machine geometry, the bending radius in the arcs is $\rho_a = \eta_d L_a / 2\pi$. We can now obtain the minimum bending radius of the arc dipoles:

$$\rho_a = \rho_i \sqrt{\frac{P_i \eta_d}{L_i \lambda_a}} \quad (12)$$

Considering a dipole filling factor of 80% in the arcs and a power density of 4 kW/m, which is comparable to existing light sources, e.g. [6], we find that each arc is 12.4 km long. The required beam current is 3A which is about twice the required current for the low energy stage of the FCC-ee [7]. Thus we consider a similar RF design, based on 400 MHz cavities. Considering the total power lost to synchrotron radiation in the insertion and the arcs, we determine the number of cavities needed, given a maximum power of 962kW per cavity [7]. Due to the high targeted power, the number of cavities is unprecedentedly high for synchrotrons: 1144. As discussed later, a voltage twice higher than the one needed to compensate for the energy loss seem appropriate in terms of bunch length and Touschek lifetime. The voltage is thus well below the maximum for these cavities [7]. The length of the RF sections is determined using the length of the FCC-ee RF modules (1.26 m) and a filling factor of 80%. We obtain a total length of 26.9 km, comparable to the LEP/LHC [8]. It includes a contingency of 200 m for the insertion, injection, extraction, cleaning and beam diagnostics.

The lattice is designed based on the LEP FODO with 90° phase advance [8], given that the targeted application does not require beam of particularly small emittance. For the same reason a vertical to horizontal emittance ratio of 5% is considered. We assume that the dispersion can be well corrected at the high field magnet, such that the radiation integrals and related beam properties can be obtained using the formulas for the FODO lattice, e.g. in [4]. We find a horizontal emittance of 0.6 nm and a bunch length of 16 ps. With these parameters and assuming that the momentum acceptance is limited only by the RF bucket height, we find a Touschek lifetime of 200h.

COST

A rough cost estimate is shown in Table 2, it is based on the empirical cost model in [9]. This model separates the

Table 2: Estimated Cost [B\$]

Beam energy	0.2
Length	3.3
RF Power	6.6
Total	10.1

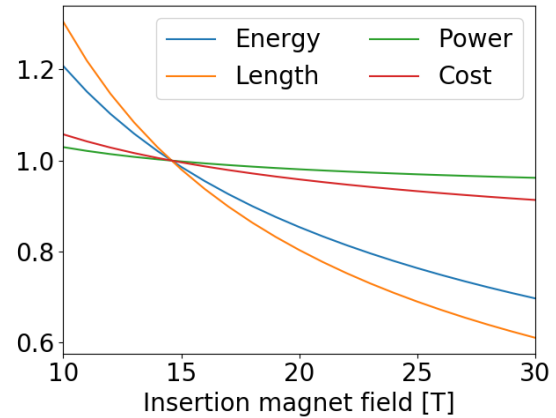


Figure 3: Scaling of the beam energy, machine length, RF power and corresponding total cost for different field of the insertion magnet. The reference is the 14.6T from the design in Table 1.

beam energy, the total length and the RF power as the main cost drivers. The unprecedentedly large power is reflected in the cost of the RF system which dominates the total cost. The R&D targeting high efficiency and low cost for the RF system of the FCC-ee is therefore highly synergetic with this concept.

The second most important cost driver is also linked to the high output power. Indeed the machine length is mostly constrained by the energy deposition in the arc (Eq. (12)). This part can be reduced using the highest field magnet for the insertion, thus featuring a synergy with the arc dipoles needed for the FCC-hh [10]. Yet the relative impact on the total cost of this contribution is rather mild, as shown by Fig. 3.

The most expensive part of the machine can easily be staged, since a reduction of the targeted power by a factor 25 (i.e. $P_i = 40MW$) would reduce equivalently this part of the cost. This implies a reduction of the number of cavities. The voltage per cavity would then reach 15 MV, remaining compatible with the FCC-ee design [7].

ACKNOWLEDGEMENTS

This study was performed in the frame of the Swiss High School Student Internship Program.

REFERENCES

- [1] F. Carminati *et al.*, “An energy amplifier for cleaner and inexhaustible nuclear energy production driven by a particle beam

- accelerator”, CERN, Geneva, Switzerland, rep. AT-93-47-ET, Nov. 1993. <https://cds.cern.ch/record/256520>
- [2] H.A. Abderrahim *et al.*, “Accelerator Driven Subcritical Systems”, *Encyclopedia of Nuclear Energy*, Oxford, UK, Elsevier, 2021, pp. 191–202. doi:10.1016/B978-0-12-819725-7.00093-3
- [3] A.V. Varlamov *et al.*, “Atlas of Giant Dipole Resonances. Parameters and Graphs of Photonuclear Reaction Cross Sections”, International Atomic Energy Agency, rep. INDC(NDS)-394, Jan 1999. https://inis.iaea.org/collection/NCLCollectionStore/_Public/30/003/30003843.pdf
- [4] A. Wolski, “Beam Dynamics in High Energy Particle Accelerators”, London, UK, Imperial College Press, 2014. doi:10.1142/p899
- [5] E. Rochepault and P. Ferracin, “CEA–CERN Block-Type Dipole Magnet for Cable Testing: FRESCA2”, *Nb₃Sn Accelerator Magnets. Designs, Technologies and Performance*, Cham, Switzerland, Springer Nature Switzerland AG, 2019, pp. 311–340. doi:10.1007/978-3-030-16118-7
- [6] L. Zhang, “Preliminary Absorber Design for the Ultimate Storage Ring Light Source”, in *Proc. EPAC’02*, Paris, France, Jun. 2002, paper WEPDO028, pp. 2592–2594.
- [7] A. Abada *et al.*, “FCC-ee: The Lepton Collider”, *Eur. Phys. J. ST.*, vol. 228, pp. 261–623, 2019. doi:10.1140/epjst/e2019-900045-4
- [8] “LEP Design report. vol 2. The LEP Main Ring”, Geneva, Switzerland: CERN, rep. LEP-84-01, June 1984. <https://cds.cern.ch/record/102083>
- [9] V. Shiltsev, “A Phenomenological Cost Model for High Energy Particle Accelerators”, *INST*, vol. 9, T07002, 2014. doi:10.1088/1748-0221/9/07/T07002
- [10] A. Abada *et al.*, “FCC-hh: The Hadron Collider”, *Eur. Phys. J. ST.*, vol. 228, pp. 775–1107, 2019. doi:10.1140/epjst/e2019-900087-0